Microvascular injuries, secondary edema, and inconsistencies in lung vascularization between affected and nonaffected pulmonary segments of non-critically ill hospitalized COVID-19 patients presenting with clinical deterioration

Cécile Maincent, Christophe Perrin, Gilles Chironi, Marie. Baqué-Juston, Frédéric Berthier, Benoît Paulmier, Florent Hugonnet, Claire Dittlot, Ryan Lukas. Farhad, Julien Renvoise, Benjamin Serrano, Valérie Nataf, François Mocquot, Olivia Keita-Perse, Yann-Erik Claessens and Marc Faraggi

Abstract

Purpose: We aimed to better understand the pathophysiology of SARS-CoV-2 pneumonia in non-critically ill hospitalized patients secondarily presenting with clinical deterioration and increase in oxygen requirement without any identified worsening factors.

Methods: We consecutively enrolled patients without clinical or biological evidence for superinfection, without left ventricular dysfunction and for whom a pulmonary embolism was discarded by computed tomography (CT) pulmonary angiography. We investigated lung ventilation and perfusion (LVP) by LVP scintigraphy, and, 24 h later, left and right ventricular function by Tc-99m-labeled albumin-gated blood-pool scintigraphy with late (60 mn) tomographic albumin images on the lungs to evaluate lung albumin retention that could indicate microvascular injuries with secondary edema.

Results: We included 20 patients with confirmed SARS-CoV-2 pneumonia. All had CT evidence of organizing pneumonia and normal left ventricular ejection fraction. No patient demonstrated preserved ventilation with perfusion defect (mismatch), which may discard a distal lung thrombosis. Patterns of ventilation and perfusion were heterogeneous in seven patients (35%) with healthy lung segments presenting a relative paradoxical hypoperfusion and hypoventilation compared with segments with organizing pneumonia presenting a relative enhancement in perfusion and preserved ventilation. Lung albumin retention in area of organizing pneumonia was observed in 12 patients (60%), indicating microvascular injuries, increase in vessel permeability, and secondary edema.

Conclusion: In hospitalized non-critically ill patients without evidence of superinfection, pulmonary embolism, or cardiac dysfunction, various types of damage may contribute to clinical deterioration including microvascular injuries and secondary edema, inconsistencies in lung segments vascularization suggesting a dysregulation of the balance in perfusion between segments affected by COVID-19 and others.

Correspondence to:
Marc Faraggi
Nuclear Medicine Department, Centre Hospitalier Princesse Grace, Avenue Pasteur, BP 480, 98012 Monaco, Monaco
marc.faraggi@chpg.mc

**Cécile Maincent
Christophe Perrin
Claire Dittlot
Ryan Lukas. Farhad
Julien Renvoise**
Pulmonary Department, Centre Hospitalier Princesse Grace, Monaco, Monaco

Gilles Chironi
Check-up Unit, Centre Hospitalier Princesse Grace, Monaco, Monaco

Marie. Baqué-Juston
Radiology Department, Centre Hospitalier Princesse Grace, Monaco, Monaco

Frédéric Berthier
Department of Biostatistics, Centre Hospitalier Princesse Grace, Monaco, Monaco

**Benoît Paulmier
Florent Hugonnet
Valérie Nataf
François Mocquot**
Nuclear Medicine Department, Centre Hospitalier Princesse Grace, Monaco, Monaco

Benjamin Serrano
Medical Physics Department, Centre Hospitalier Princesse Grace, Monaco, Monaco

Olivia Keita-Perse
Department of Infectious disease, Centre Hospitalier Princesse Grace, Monaco, Monaco

Yann-Erik Claessens
Department of Emergency Medicine, Centre Hospitalier Princesse Grace, Monaco, Monaco

Summary Statement

Microvascular injuries and dysregulation of the balance in perfusion between segments affected by COVID-19 and others are present in non-critically ill patients without other known aggravating factors.

Key Results

In non-critically ill patients without evidence of superinfection, pulmonary embolism, macroscopic distal thrombosis or cardiac dysfunction, various types of damage may contribute to clinical deterioration including 1/ microvascular injuries and secondary edema, 2/ inconsistencies in lung segments vascularization with hypervascularization of consolidated segments contrasting with hypoperfusion of not affected segments, suggesting a dysregulation of the balance in perfusion between segments affected by COVID-19 and others.

Introduction

The causes for clinical deterioration and increase in oxygen requirement in hospitalized patients with SARS-CoV-2 pneumonia remain uncertain. The extent of lung involvement assessed by computed tomography (CT) has been reported as a prognostic factor, still many patients exhibit a moderate extent but require admission to an intensive care unit while others present a larger extent but remain clinically stable.[1,2]

To explain these puzzling discordances between clinical presentation and imaging, a wide use of CT pulmonary angiography (CTPA) has been proposed to detect possible pulmonary embolism despite the unclear risk of venous thromboembolism.[3,4]

Other hypotheses have emerged, including a vasculitis/endothelitis and thrombo-inflammatory process[5–7] potentially associated with local peripheral thrombosis undetected by conventional CTPA. This « vasculocentric » approach is consistent with the observation of arterial vessels enlargement at CT[8,9] and the potential loss of hypoxemia-related vasoconstriction in infected tissues.[8,10] Furthermore, a loss of distal microvasculature and scars of intra-alveolar deposit of fluid, fibrin and hyaluran, disrupted alveolar capillaries with platelet-fibrin microthrombi[10–13] were also reported in pathology series.[10–12] However, these autopsy findings that reported endothelitis and alveolitis[10,11] were performed in ultimately ill SARS-CoV-2 pneumonia but it is unclear if these damages may also occur in non-critically ill patients although suggested in one pathologic study of two cases who underwent lung lobectomies for adenocarcinoma and were retrospectively found to have had COVID-19 at the time of the operation.[12] Furthermore, the reduction of distal microvasculature does not necessarily imply microvessel thrombosis, as the inflammatory process itself may explain the (micro)vasculature impairment and may lead to an increase of vessel permeability, interstitial edema, elevation of interstitial pressure, and external compression of the vessels' lumen, finally resulting in a drop of oxygen transportation and arterial blood flow. To our knowledge, such an edema in non-critically ill patients has never been evidenced in vivo. In addition, studies of CTPA combined with artificial intelligence[13,14] have shown a lessering of pulmonary microvessels (below 5 mm²) in patients with COVID-19 as well as in community-acquired pneumonia, this decrease being a prognostic factor for the risk of mechanical ventilation or death.[13]

To better understand the complex relationships between alveolar ventilation, pulmonary vascularization and interstitial edema related to abnormal permeability, we prospectively investigated non-critically ill COVID-19 patients admitted for a sudden clinical deterioration, or suddenly worsening during hospitalization, without clinical evidence for other pathological process. Lung ventilation/perfusion was evaluated by lung ventilation/perfusion scintigraphy (LVPS) and

Tc-99m-labeled albumin-gated blood-pool scintigraphy (GBPS) was used for evaluation of left and right ejection fraction (LVEF and RVEF) and detection of interstitial edema related to abnormal capillar permeability.

Materials and methods

Patients

From February to September 2021, we prospectively included non-critically ill patients hospitalized in the COVID-19 unit of our institution (1) presenting with a sudden clinical deterioration defined by a respiratory rate impairment and a rise of oxygen flow to reach a peripheral capillary oxygen saturation (SpO2) of more than 95% during at least 48h, (2) for whom a diagnosis of pulmonary embolism was discarded by CTPA, (3) without clinical or biological evidence for pulmonary superinfection, and (4) without evidence for left ventricular (LV) dysfunction (Figure 1).

COVID-19 was confirmed according to the World Health Organization (WHO) guidance[15] by a positive result of reverse transcription-polymerase chain reaction (RT-PCR) assay of nasal swabs, peripheral pulmonary ground-glass opacities (GGO), or air-space consolidation on their chest CT scan at admission and suggestive common laboratory findings.[16] Patients could not be included if their medical condition was unstable, if they were under mechanical ventilation or required critical care unit, in case of clinical evidence for lung superinfection or heart failure or in case of a pregnancy. Personal protective equipment was available for the staff, and all measures to ensure strict infection prevention were observed according to established guidance.[17] The institutional review board for human studies approved the protocol and a written consent was obtained from all patients. The protocol was registered in Clinical Trials Registry.

Chest CT and CTPA

Chest CT scan was performed with blocked inspiration using an Aquilion ONE PRISM (Canon Medical Systems, Okinawa, Japan) and the following parameters: tube voltage of 120 kVp and an automatic tube current modulation (SUREexposure®), rotation time 0.5 s, pitch factor 0.81. Axial reconstructions were performed with a matrix size 512×512 with a hard
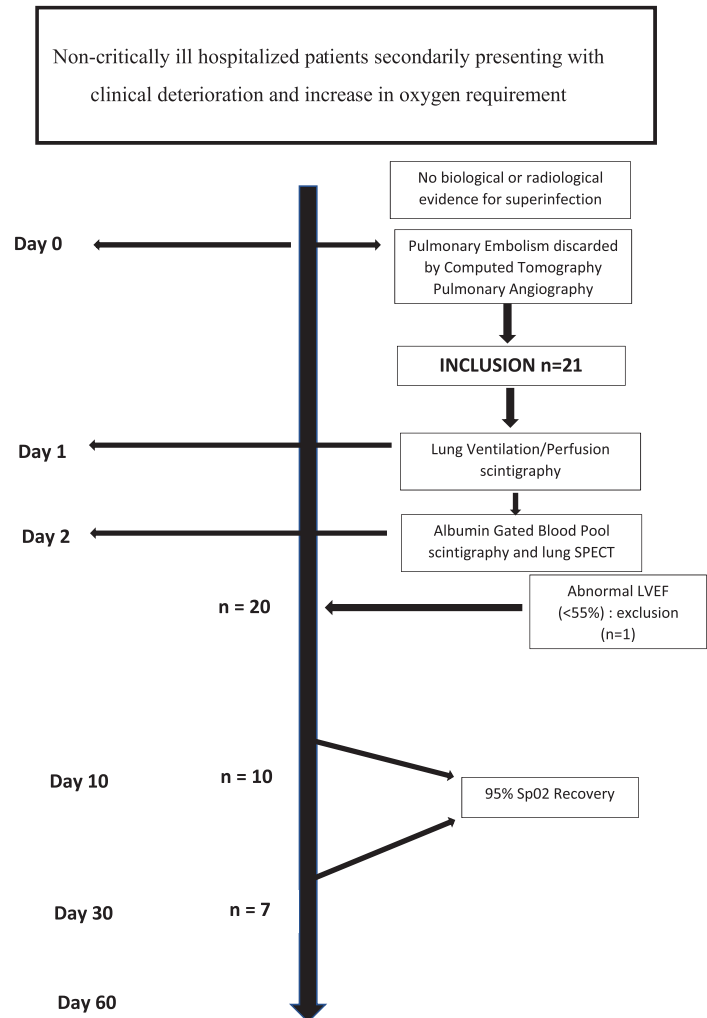

Figure 1. Patients' flow diagram.
LVEF, left ventricular ejection fraction; SPECT, single photon emission computed tomography.

convolution kernel FC35, appropriate for lung exploration, with 1 mm slice thickness and 0.8 mm slice spacing. The same procedure was used after contrast agent administration with a hard convolution kernel « bodysharp » 1 mm/0.8 mm and intravenous administration of Optiject 350 (Guerbet, Villepinte, France), 50 ml at a flow of 4 ml/s.

LVPS

LVPS imaging was performed within 24 h after CTPA, in accordance with the recommendations

of the European Association of Nuclear Medicine using a large field-of-view dual-head gamma-camera with a low-energy, all-purpose collimator (WEHR45) was used (Discovery NM/CT 870 CZT General Electric). Between 370 and 420 MBq of Technegas® (Cyclomedica Ltd, Kingsgrove, NSW, Australia) was prepared for inhalation and ventilation tomography was performed thereafter.[18–20] Then, while the patient was carefully maintained in the same supine position, 185 MBq Tc-99m-macroaggegates (Pulmocis; Curium, Paris, France) were slowly injected intravenously followed by the perfusion tomography.[20,21]

All acquisitions were performed with body contour (128 × 128 matrix, zoom 1, 60 projections over 360°, 20 s duration for ventilation and 15 s for the perfusion study) and reconstructed (10 subsets, 2 iterations, resolution recovery option).

A combined CT acquisition was performed (120 kV, intensity modulation, rotating time 0.7 s, pitch 1.375, matrix size 512 × 512, slice thickness 2.5 mm/2.5 mm).

The ventilation study was performed in a room specifically dedicated for this activity and reserved for COVID-19 patients at the end of the daily program and then room and materials were fully cleaned and sterilized according to the institutional procedures.

Tc-99m-albumin GBPS
The day following LVPS, 740 MBq of Tc99m-labeled albumin (Vasculocis 10 mg, CIS-BIO International, Gif sur Yvette, France) was intravenously administered.

Cardiac GBPS was then performed in best septal left anterior oblique (around 30°) and left lateral according to the following parameters: 128 × 128 matrix, 5000 Kcts, 16 bin zoom ×2. LVEF and RVEF were automatically computed using a dedicated software (XTERNA, Xelerix 3, General Electric).

In 45 to 60 min after IV administration, a non-gated tomographic acquisition over the lungs was performed, with the same parameters than for LVPS SPECT, resulting in a late albumin acquisition (Alb).

Scintigraphic data management

Visual analysis
Visual analysis was performed on a segmental level. Only segments with involvement of more than 50% were considered. According to the ventilation and perfusion pattern, each segment was classified into (1) 'normal' when lung ventilation (LV) and lung perfusion (LP) demonstrated a normal and homogeneous uptake, (2) 'abnormal and matched' when both LV and LP were similarly altered, (3) 'regularly mismatched' in case of hypoperfusion but normal ventilation, and (4) 'reversely mismatched' in case of hypoventilation but normal perfusion.

Furthermore, perfusion and ventilation of COVID-19 involved area were compared with those of 'normal' area to detect the presence of paradoxically hypoperfused and hypoventilated normal segments. For quantitative analysis, area with patent emphysema on CT was systematically excluded.

Quantitative analysis of GBPS data
On the CT acquired with LVPS, several volume of interest (VOIs) were drawn over one area free of CT, perfusion and ventilation abnormalities (reference area), and over the most significant COVID-19 CT abnormalities (GGO or organizing pneumonia). These VOIs were reported on each scintigraphic acquisition. An index of pathological uptake was then defined for each method as the ratio of the mean counts value in the pathological VOI over the mean counts value in the normal reference area, defining 3 indexes: ventilation index (VI), perfusion index (PI), and albumin index (AI). In healthy patients, PIs obtained by PI and AI are very close but may differ in case of lung/perfusion heterogeneity from one area to another or according to the pathology involved. Based on a personal unpublished series of 12 patients presenting with cardiogenic pulmonary edema, free of pulmonary infection and investigated by both LVPS (to discard pulmonary embolism) and GBPS (to evaluate LVEF), an albumin retention was considered significant when the ratio AI/PI was equal or above 1.7 (mean value + 2 standard deviation: 1.26 + 0.21, Table 1).

Patients' short-term clinical outcome
Follow-up was continued either as long as patients demonstrated a 95% SpO2 recovery in ambient

Table 1. Determination of a significant AI/PI ratio.

Patient	LVEF	AI/PI
1	47	1.15
2	24	1.55
3	37	1.45
4	50	1.02
5	41	1.2
6	33	1.35
7	45	1.31
8	49	0.95
9	49	0.92
10	29	1.48
11	36	1.38
12	40	1.3
mean	40.25	1.26
SD	8.79	0.21

AI/PI, Albumin index/perfusion index; SD, standard deviation.
Unpublished data of 12 patients presenting with cardiogenic pulmonary edema, free of pulmonary infection. Patients were investigated by both lung ventilation/perfusion scintigraphy to discard pulmonary embolism that could have induced cardiac dysfunction, and gated blood-pool scintigraphy to evaluate left ventricular ejection fraction (LVEF). AI/PI was calculated as described in the methodology section for the COVID-19 patients. A non-cardiogenic albumin uptake was considered significant when the ratio AI/PI was equal or above 1.7 (mean value + 2 standard deviation).

air or at least 10 days for patients with residual O2 therapy.

Patients' short-term clinical outcome during hospitalization was classified as follows: improvement, worsening, stability, or long COVID by an adjudication committee consisting of three physicians experienced in intensive care, pulmonology, and emergency medicine and involved in the management of COVID-19 patients. The expert panel was blinded to the results of LVPS but had full access to medical records, focusing on the kinetics of monitoring, treatment (notably oxygen delivery), and biology from 3 days before to 4 days after LVPS.

Statistical management

Categorical variables were collected as numbers (*n*) and percentages (%). Continuous variables were described as median and interquartile range (IQR).

Prognosis was evaluated using categorical variables: worsening or stability *versus* improvement in the 15 following days, delay to the recovery of a 95% or more SpO2 in ambient air below *versus* above 15 days, hospitalization duration below *versus* above 15 days.

The prognostic value of the extent of CT abnormalities, an RVEF below *versus* above 50%, a significant albumin uptake (AI/PI) above or equal to 1.7, and the presence and/or number of paradoxically hypoventilated and hypoperfused normal segments were evaluated by Fisher's exact test and Mann–Whitney *U* test.

Results

Patients

Twenty-one patients were prospectively included; one was secondarily excluded because of abnormal LVEF. Population characteristics are summarized in Table 2. The 13 first patients were infected with the B 1.1.7 variant, the 7 remaining with the Delta variant.

No patient received oxygen therapy before hospitalization except patient no. 2 who received long-term oxygen therapy (2 l/min) for chronic obstructive pulmonary disease.

Thirteen patients were included because they required an increase in oxygen delivery from baseline status, two because a pulmonary thrombosis was suspected because of sudden hypoxemia and d-dimer increase (patients 6 and 8), five because oxygen therapy could not be withdrawn despite a moderate or stable involvement at CT.

All patients received 6 mg of dexamethasone, anticoagulant therapy doses were prophylactic in 13 patients, and full intensity in 7 (2 because of a past history of venous thromboembolism: patients 9 and 12). Only two patients received anti-IL6-R therapy (tocilizumab, patients 1 and 3). No patient experienced any secondary lung bacterial infection, one had an elevated leucocyte count related

Table 2. Patients' clinical characteristics.

Patient no.	Age (y) / Gender	Delay to clinical deterioration since symptom onset (d)	Respiratory rate (/min)	Increment in O2 (l/min)	Hospitalization duration (d)	Extent of COVID involvement at baseline CT (%)	Comorbidity	Delay to 95% SpO2 recovery (d)/residual O2 therapy (l/min)	Clinical evolution
1	77/M	12	24	6	32	20	HT, FA	>60/1	W (ICU)
2	80/M	10	16	7	28	10	COPD, CAD, RD, HT	60/0	S
3	54/M	24	16	5	20	70	BMI, HT	>60/1	I
4	87/M	15	22	5	45	40	CAD	60/0	S
5	61/F	13	21	1	8	20	HT	4/0	I
6	68/F	15	20	5	16	30	BMI	13/0	S
7	85/M	9	28	6	16	40	HT, BMI, DM	>60/1	I
8	79/M	10	16	2	6	15	DM, AF, HT, CAD	4/0	I
9	61/M	14	22	4	10	25	0	10/0	I
10	52/M	10	24	5	10	20	0	9/0	I
11	86/M	15	12	4	10	60	HT	9/0	I
12	40/M	10	22	5	10	60	BMI, Asth	9/0	I
13	54/M	12	20	1	5	10	BMI, CAD, Asth	3/0	I
14	52/F	4	34	4	7	60	BMI	6/0	I
15	50/F	7	20	HFNC	30	50	BMI	>30/2	LC
16	69/F	15	16	HFNC	44	70	0	>40/2	LC
17	48/F	16	20	3	9	75	BMI	10/2	I
18	65/M	14	18	HFNC	15	90	BMI	16/2	I
19	68/M	11	18	2	5	30	HTA	4/0.5	I
20	44/M	16	20	3	7	25	BMI	5/0	i
Median[a]	63	12.5	20	5	16.5	35	–	10/0	W S LC: 6 (30%)
IQR[a]	26	5	5	3		40	–	45/1	I: 14 (70%)

0, none; AF, atrial fibrillation; Asth, asthma; BMI, body mass index >30; CAD, coronary artery disease; CT, computed tomography; DM, diabetes mellitus; F, female; HFNC, high-flow nasal cannula (60 l/min); HT, hypertension; I, improvement; ICU, intensive care unit; IQR, interquartile range; LC, long COVID; M, male; RD, renal dysfunction; S, stability; SpO2, peripheral capillary hemoglobin oxygen saturation; W, worsening.
[a]Median/IQR or number and percentage if appropriate.

to a urinary infection (patient 16). The extent of CT abnormalities ranged from 10 to 90%.

The delay to recovery of a 95% or more SpO2 in ambient air was 15 days or less in 12 patients. Nine patients were hospitalized for 15 days or more. Biological data are summarized in Table 3.

LVPS

No patient demonstrated pulmonary segments or subsegments with both preserved ventilation and hypoperfusion (mismatch) that could be suggestive of macroscopic distal thrombosis.

Perfusion and ventilation patterns were very heterogeneous from one patient to another but also within a same patient, among whom different patterns coexisted. Patterns are summarized in Table 3.

Three patients had normal LVPS. Seven patients (35%) without past history of asthma demonstrated paradoxical concordant segments with a relative hypoperfusion and hypoventilation in areas visually free from COVID19-involvement, whereas COVID19-involved segments demonstrated a relative hyperperfusion with preserved ventilation. In one case, a peripheral halo of hyperperfusion surrounding the COVID-19 involvement was seen on LVPS (Figure 2).

Three patients had tracheobronchial tract uptake of Technegas.

GBPS

Twelve patients (60%) showed a significant late pulmonary uptake of albumin in at least one COVID-19 area (Table 2 and Figures 3 and 4).

All patients had a normal LVEF (above 55%), while 11 had a decreased RVEF (below 50%).

Clinical evolution

Procalcitonin level was the only significant factor related to the duration of hospitalization (clinical improvement *versus* others: 0.06 mg/l, IQR = 0.06 [0.03-0.17] *versus* 0.13 mg/l, IQR = 0.05 [0.06-0.78], $p = 0.04$) or to the delay to 95% SpO2 recovery (<15 days *versus* others: 0.06 mg/l, IQR = 0.04 [0.04-0.12] *versus* 0.13 mg/l, IQR = 0.06 [0.03-0.78], $p = 0.03$).

Table 3. Patients' biological and scintigraphic data.

Patient no.	CRP (mg/l)	Fibrinogen (g/l)	d-dimer (mg/l)	Leucocyte / neutrophil counts ($10^3/\mu$l)	Platelet counts ($10^3/\mu$l)	Procalcitonin (mg/l)	LVEF (%)	RVEF (%)	Scintigraphic pattern (number of segments)	AI/PI	Albumin uptake
1	45.6	4.67	228	8.32/7.08	158	0.13	59	40	M (1), RMI (1), PMN (0), N(18)	2.9	+
2	93.2	7.29	2007	5.51/5.20	264	0.78	75	71	M (7), RMI (2), PMN (3), N(8)	1.9	+
3	0.6	2.26	437	6.68/5.31	218	0.03	58	55	M (2), RMI (0), PMN (0), N(18)	2.3	+
4	75.3	4.34	6758	6.89/5.71	211	0.15	60	55	M (0), RMI (0), PMN (0), N(20)	1.5	–
5	8.2	3.60	762	4.72/2.98	218	0.10	72	45	M (2), RMI (0), PMN (0), N(18)	14.4	+
6	26.3	4.53	782	10.63/7.85	287	0.06	64	60	M (0), RMI (5), PMN (0), N(15)	1.8	+
7	178.0	6.08	4360	6.39/4.98	288	0.17	59	67	M (1), RMI (0), PMN (7), N(12)	1.3	–
8	41.5	4.74	1511	3.46/2.74	127	0.11	56	39	M (0), RMI (0), PMN (0), N(20)	2.3	+

(Continued)

Table 3. (Continued)

Patient no.	CRP (mg/l)	Fibrinogen (g/l)	d-dimer (mg/l)	Leucocyte / neutrophil counts (10³/µl)	Platelet counts (10³/µl)	Procalcitonin (mg/l)	LVEF (%)	RVEF (%)	Scintigraphic pattern (number of segments)	AI/PI	Albumin uptake
9	6.2	4.29	785	8.70/6.45	307	0.05	62	36	M (0), RMI (0), PMN (2), N(18)	1.7	+
10	19.0	3.50	1288	8.84/7.29	151	0.06	58	49	M (0), RMI (0), PMN (0), N(20)	1.5	–
11	20.9	3.64	655	9.09/6.74	382	0.07	63	49	M (2), RMI (0), PMN (3), N(15)	1.5	–
12	118.0	6.88	509	4.29/3.58	207	0.12	60	43	M (1), RMI (3), PMN (0), N(16)	1.7	+
13	1.7	3.51	215	7.73/5.38	235	0.04	65	64	M (1), RMI (0), PMN (0), N(19)	1.8	+
14	11.9	4.3	512	9.18/6.31	440	0.04	67	51	M(0), RMI(2), PMN(0), N(18)	1	–
15	30.3	4.48	673	6.88/5.50	266	0.1	56	36	M(10), RMI(0), PMN(0), N(10)	2	+
16	18	4.0	526	13.37/12.47	235	0.12	66	65	M(0), RMI(0), PMN(8), N(12)	0.9	–
17	18	5.16	335	6.57/4.47	268	0.05	57	37	M(6), RMI(0), PMN(0), N(14)	0.6	–
18	72	6.55	875	9.44/7.46	382	0.1	70	34	M(0), RMI(0), PMN(3), N(17)	1.9	+
19	107	7.1	755	5.49/4.50	358	0.04	61	54	M(4), RMI(0), PMN(0), n(16)	1.6	–
20	15.6	3.82	228	10.83/7.83	399	0.06	55	43	M(3), RMI(2), PMN(4),N(11)	1.7	+
Median[a]	23.6	4.41	714	7.31/5.61	265	0.09	60.5	49	M(1), RMI(0), PMN (0), N16	1.7	+: 12 (60%)
IQR	59.9	1.89	608.5	3.19/2.45	118	0.07	7.5	18	M(2.5), RM(1.5), PMN(3), N(5.5)	0.45	–: 8 (40%)

AI/PI, albumin index/perfusion index; CRP, C-reactive protein; IQR, interquartile range; LVEF, left ventricular ejection fraction; M, match (segments with concordant altered perfusion and ventilation); N, normally perfused and ventilated segments; PMN, paradoxically matched (relatively hypoperfused and hypoventilated normal segments); RMI, reverse mismatch (hypoventilated segments with preserved perfusion); RVEF, right ventricular ejection fraction.
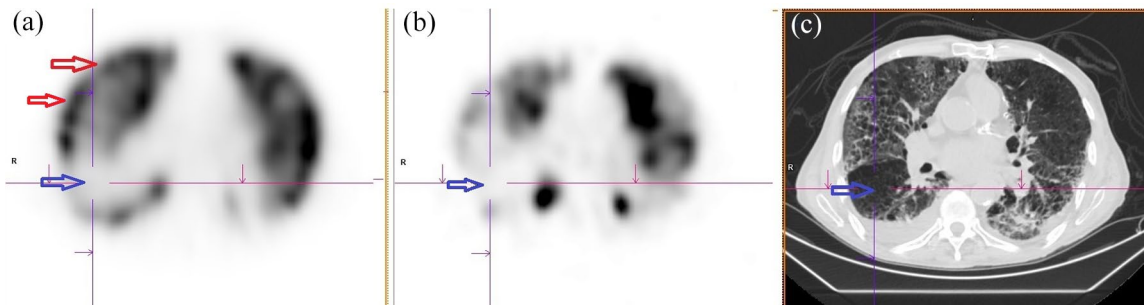[a]Median/IQR or number and percentage if appropriate.

Figure 2. Patient no. 2. Perfusion (a), ventilation (b), and CT scan (c). Blue arrow: non-COVID-19-involved area of the right Fowler lobe, with paradoxically matched hypoperfusion and hypoventilation, while the COVID-19-involved area of the right superior lobe just in front remains perfused with a slightly hyperperfused peripheral halo (red arrow).
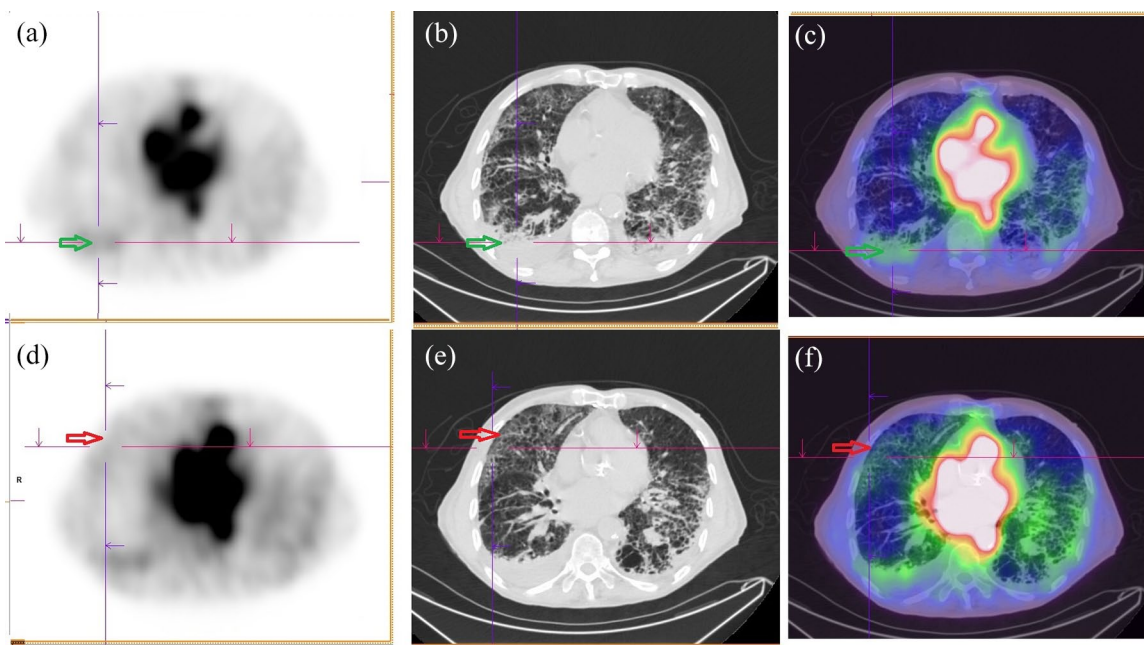

Figure 3. Patient no. 2. Albumin (a), CT (b), and fused CT + albumin scan (c). Green arrow: COVID-19 condensation of the right base with significant albumin uptake and moderate pleural effusion behind. There is also a moderate albumin uptake of the left inferior lobe. Albumin (d), CT (e), and fused CT + albumin scan (f). The moderate albumin uptake in the area of the peripheral halo of the COVID-19-involved area in the right superior lobe (red arrow) is related to the corresponding hyperperfusion displayed in Figure 2 (red arrow).

Discussion

Among non-critically ill patients with CT evidence of SARS-CoV-2-related organizing pneumonia, our study evidences (1) the presence of lung albumin retention in some COVID-19-involved areas indicating microvascular injuries, vessel permeability increase, and secondary edema; (2) the absence of any ventilation/perfusion mismatch, which may discard macroscopic distal thrombi; and (3) ventilation and perfusion abnormalities within 35% of patients several healthy lung segments demonstrating a relative hypoperfusion and hypoventilation while segments with organizing pneumonia appeared relatively hyperperfused.

The injection of microspheres upstream in an organ is a reference experimental method to measure downstream tissular blood flow. For a clinical use, lung perfusion scintigraphy is considered the best method to detect small distal pulmonary embolism and its results can be considered as a
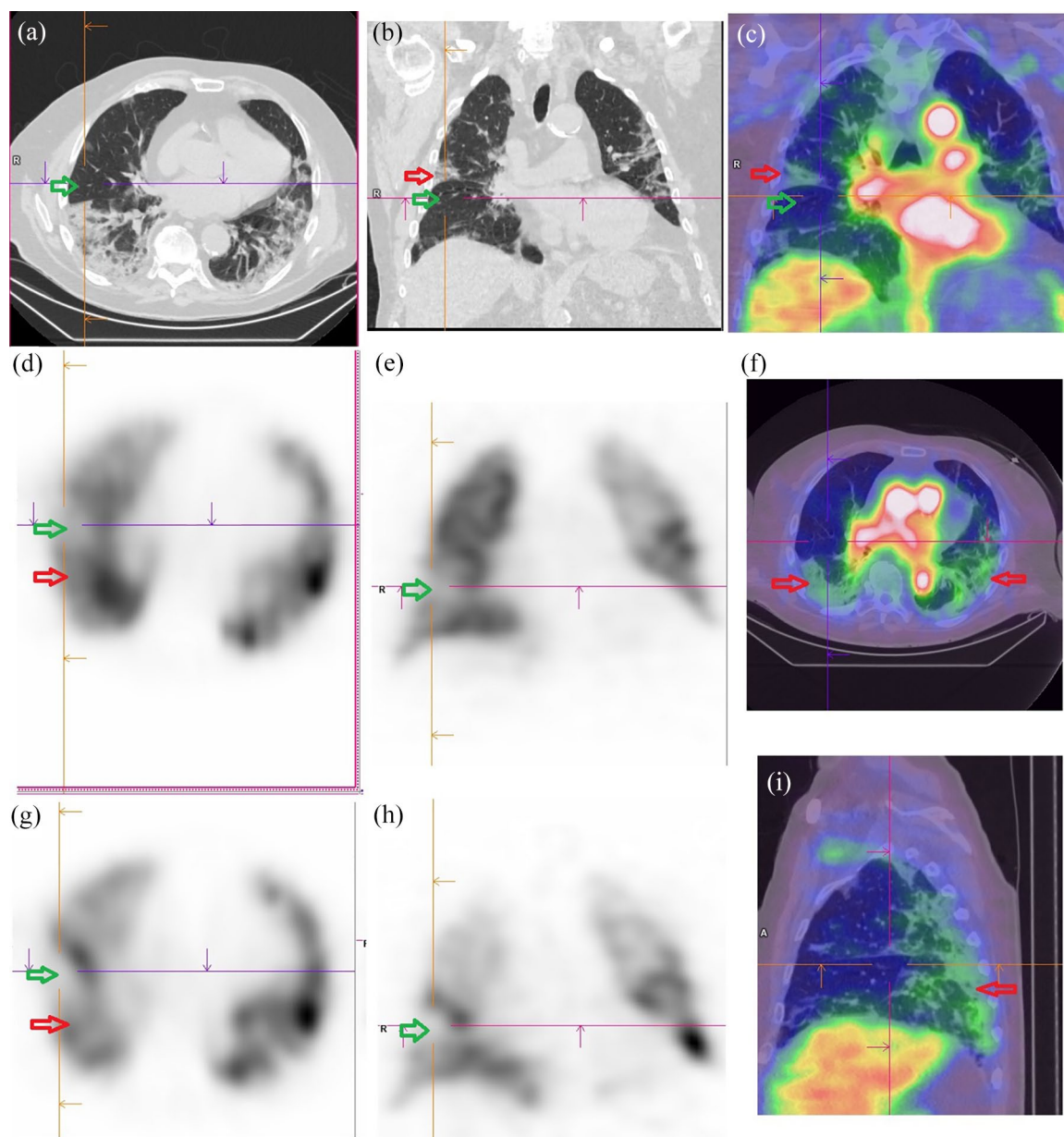
Figure 4. Patient no. 7. Axial (a) and coronal CT slices (b). Corresponding perfusion (d, e) and ventilation (g, h) scans. Corresponding coronal (c), axial (f), and saggital (i) fused albumin and CT scans. Green arrow: non-COVID-19-involved segment of the right inferior lobe, with paradoxically matched hypoperfusion and hypoventilation, while the COVID-19-involved area just behind (red arrow) is normally ventilated and perfused. (c), (f), (i): Red arrow: significant albumin uptake in several COVID-19-related condensed areas.

surrogate of lung vascularization evaluation. 99m-Tc Technegas is the best aerosol particularly in patients with chronic obstructive pulmonary disease as, because of the very small particle size, this agent is distributed in the lungs almost like a gas and deposited in alveoli by diffusion, where they remain stable. LVPS has been previously used in SARS-CoV-2 pneumonia to discard pulmonary embolism when CTPA was not indicated[22–24] or to evidence tracheobronchitis.[25] Furthermore, in case of normal CTPA and typically abnormal LVPS (i.e. area with preserved ventilation and perfusion defect), impairment of distal vasculature might be detected whatever the mechanism (very distal and small pulmonary embolism or local thrombosis). Another way to evaluate local

pulmonary vasculature is to use an intravascular tracer that is not supposed to escape out of the vessel. Because of a high molecular weight (around 70,000 Da), Tc-99m-labeled albumin fulfills this criterion. Therefore, it might be expected that LP scintigraphy and Tc-99m-albumin exhibit concordant data about pulmonary arterial blood flow. In case of an enhanced uptake of albumin in COVID-19-involved areas compared with LP estimation of the blood flow, as evaluated by the AI/PI ratio, a leakage of albumin out of the pulmonary capillaries as a consequence of abnormal capillaries permeability and endothelial dysfunction could be strongly suggested, as it has been described both in acute respiratory distress syndrome (ARDS) and in genetically modified mice permanently expressing the human angiotensin-converting enzyme 2 receptor (ACE2) and infected with SARS-CoV-2.[26] These capillary injuries, usually described in very severe clinical presentations, might occur in moderate to mild COVID-19 patients (as ours) with a preserved good prognosis.

In several clinical and histopathological models of tissue inflammation, interstitial and peri-vascular edema impairs the functional vascularization and tissue oxygen delivery,[27] whatever the amount of microvessels involved. As the oxygen delivery is driven by a facilitated diffusion mechanism (the combination of a concentration and a pressure gradient), what increases the interstitial pressure decreases the oxygen diffusion throughout the microvessel walls. In other words, it is not surprising that the participation of microvessel damage–related edema, evidenced by Tc-99m-labeled albumin, could be an exacerbating factor for hypoxemia.

However, even in the same patient, areas with CT consolidation may demonstrate albumin uptake or not. As the albumin diffusion flux throughout the injured vessels may be reduced when the interstitial pressure increases, this apparent discrepancy might be explained by the coexistence of lesions of different ages and/or evolutionary phase.

One intriguing finding is that some supposed normal areas (i.e. looking free of COVID-19 involvement at CT) appeared less perfused and less ventilated than COVID-19-related 'healed' areas that present normal or enhanced perfusion. In LVPS, in the absence of pulmonary embolism, most of these latter segments should rather appear

both hypoventilated and hypoperfused, which would be consistent with (1) the filling of alveoli and alveolar ducts with fibrinous, spindle-shaped fibroblasts and myofibroblasts that later form granulation tissue seen in organizing pneumonia[1,28] and/or COVID-19[5] and (2) with the interstitial edema perturbating the microvasculature function. These normally or relatively hyperperfused segments (compared with healthy segments) are very different from the typical inflammatory peripheral halo around SARS-CoV-2 pneumonia areas described on dual-energy CT[8] and shown in Figure 2 on which the hypervascularization affects the boundaries of these lesions and not the core of the CT consolidation area.

The relative hypoventilation and hypoperfusion of noninvolved segments may also suggest direct bronchoconstriction and vasoconstriction as no mucous plugging was observed by LVPS in these paradoxical segments to suspect an adaptative vasoconstriction. Bronchial constriction out of pathological segments has been known from decades for pulmonary embolism.[29–31] Vasoconstriction might also be a secondary effect of the SARS-CoV-2 virus action, which targets the ACE2 receptor and then perturbates the local renin/angiotensin regulation.[26,32] At the beginning of viral invasion by SARS coV-2, it has been suggested that the initial hyperhemia inducing alveolar damage in affected segments might be associated with a loss of local hypoxic vasoconstriction,[6,26,33,34] leading to a right-to-left shunt effect.

Study limitation

We deliberately chose to enroll very selected COVID-19 patients, with the fewest confounding factors (i.e. pulmonary embolism, heart failure), to better understand the clinical deterioration of non-critically ill patients. The worldwide pandemy of SARS-CoV-2 pneumonia raised physiopathological questions that were also probably relevant for other forms of ARDS and/or organized pneumonia. Unfortunately, those forms of ARDS were not similarly investigated. We were not able to include a control group of non-COVID-19 patients, and, to our knowledge, nobody reported combined lung perfusion/ventilation and albumin uptake studies in non-COVID-19 ARDS. Nevertheless, it is likely that our results

are not specific to SARS-CoV-2 pneumonia and might be found in ARDS related to other pneumonia. Further studies with larger series must be driven to compare COVID-19 and non-COVID-19 ARDS and to better assess prognostic factors.

Conclusion
In non-critically ill patients hospitalized for COVID-19 presenting with an increase in oxygen requirement and without any evidence for pulmonary artery embolism, LV dysfunction or lung superinfection, we observed (1) an albumin retention in some consolidated COVID segments in 60% of patients, suggesting microvasculature/alveolar-epithelial barrier damage and (2) inconsistencies in lung segments vascularization in 35% of patients suggesting a dysregulation of the balance in perfusion between segments affected by COVID-19 and others.

Ethics approval, consent to participate and for publication
The institutional review board for human studies approved the protocol and a written consent was obtained from the subjects.

Author contribution(s)
Cécile Maincent: Investigation; Writing – original draft.

Christophe Perrin: Resources; Supervision; Validation.

Gilles Chironi: Resources; Supervision; Validation.

Marie. Baqué-Juston: Data curation; Resources.

Frédéric Berthier: Formal analysis; Methodology.

Benoît Paulmier: Resources; Visualization.

Florent Hugonnet: Investigation; Resources; Visualization.

Claire Dittlot: Data curation; Resources.

Ryan Lukas. Farhad: Investigation; Resources.

Julien Renvoise: Investigation; Resources.

Benjamin Serrano: Resources; Software.

Valérie Nataf: Investigation; Resources.

François Mocquot: Resources.

Olivia Keita-Perse: Investigation; Resources; Supervision.

Yann-Erick Claessens: Conceptualization; Supervision; Validation; Writing – review & editing.

Marc Faraggi: Conceptualization; Methodology; Supervision; Writing – review & editing.

ORCID iD
Marc Faraggi [iD] https://orcid.org/0000-0002-7233-1410

Conflict of interest statement
The authors declared no potential conflicts of interest with respect to the research, authorship, and/or publication of this article.

Clinical Trials Registry Number
NCT04990505.

References

1. Kory P and Kanne JP. SARS-CoV-2 organising pneumonia: 'Has there been a widespread failure to identify and treat this prevalent condition in COVID-19? *BMJ Open Respir Res* 2020; 7: e000724.

2. Tobin MJ, Laghi F and Jubran A. Why COVID-19 silent hypoxemia is baffling to physicians. *Am J Respir Crit Care Med* 2020; 202: 356–360.

3. Roubinian NH, Dusendang JR, Mark DG, *et al.* Incidence of 30-day venous thromboembolism in adults tested for SARS-CoV-2 infection in an integrated health care system in Northern California. *JAMA Intern Med* 2021; 181: 997–1000.

4. Jimenez D, Garcia-Sanchez A, Rali P, *et al.* Incidence of VTE and bleeding among hospitalized patients with coronavirus disease 2019: a systematic review and meta-analysis. *Chest* 2021; 159: 1182–1196.

5. Afshar-Oromieh A, Prosch H, Schaefer-Prokop C, *et al.* A comprehensive review of imaging findings in COVID-19 – status in early 2021. *Eur J Nucl Med Mol Imaging* 2021; 48: 2500–2524.

6. Sadegh Beigee F, Pourabdollah Toutkaboni M, Khalili N, *et al.* Diffuse alveolar damage

and thrombotic microangiopathy are the main histopathological findings in lung tissue biopsy samples of COVID-19 patients. *Pathol Res Pract* 2020; 216: 153228.

7. Magro C, Mulvey JJ, Berlin D, *et al.* Complement associated microvascular injury and thrombosis in the pathogenesis of severe COVID-19 infection: a report of five cases. *Transl Res* 2020; 220: 1–13.

8. Lang M, Som A, Mendoza DP, *et al.* Hypoxaemia related to COVID-19: vascular and perfusion abnormalities on dual-energy CT. *Lancet Infect Dis* 2020; 20: 1365–1366.

9. Osuchowski MF, Winkler MS, Skirecki T, *et al.* The COVID-19 puzzle: deciphering pathophysiology and phenotypes of a new disease entity. *Lancet Respir Med* 2021; 9: 622–642.

10. Varga Z, Flammer AJ, Steiger P, *et al.* Endothelial cell infection and endotheliitis in COVID-19. *Lancet* 2020; 395: 1417–1418.

11. Carsana L, Sonzogni A, Nasr A, *et al.* Pulmonary post-mortem findings in a series of COVID-19 cases from northern Italy: a two-centre descriptive study. *Lancet Infect Dis* 2020; 20: 1135–1140.

12. Tian S, Hu W, Niu L, *et al.* Pulmonary pathology of early-phase 2019 novel coronavirus (COVID-19) pneumonia in two patients with lung cancer. *J Thorac Oncol* 2020; 15: 700–704.

13. Morris MF, Pershad Y, Kang P, *et al.* Altered pulmonary blood volume distribution as a biomarker for predicting outcomes in COVID-19 disease. *Eur Respir J* 2021; 58: 2004133.

14. George PM and Desai SR. COVID-19 pneumonia and the pulmonary vasculature – a marriage made in hell. *Eur Respir J* 2021; 58: 2100811.

15. WHO. Clinical management of severe acute respiratory infection when novel coronavirus (nCoV) infection is suspected: interim guidance, 2020, https://apps.who.int/iris/handle/10665/330854 (accessed 15 June 2021).

16. Maincent C, Berthier F, Fahrad RL, *et al.* Accuracy of routine biomarkers and blood leucocytes count to assist diagnosis of COVID-19-associated pneumonia in adult patients visiting the emergency department. *Res Square* 2021, https://www.researchsquare.com/article/rs-34817/v1

17. Paez D, Gnanasegaran G, Fanti S, *et al.* COVID-19 pandemic: guidance for nuclear medicine departments. *Eur J Nucl Med Mol Imaging* 2020; 47: 1615–1619.

18. Bajc M, Neilly JB, Miniati M, *et al.* EANM guidelines for ventilation/perfusion scintigraphy: part 1. Pulmonary imaging with ventilation/perfusion single photon emission tomography. *Eur J Nucl Med Mol Imaging* 2009; 36: 1356–1370.

19. Bajc M, Neilly JB, Miniati M, *et al.* EANM guidelines for ventilation/perfusion scintigraphy: part 2. Algorithms and clinical considerations for diagnosis of pulmonary emboli with V/P(SPECT) and MDCT. *Eur J Nucl Med Mol Imaging* 2009; 36: 1528–1538.

20. Bajc M, Chen Y, Wang J, *et al.* Identifying the heterogeneity of COPD by V/P SPECT: a new tool for improving the diagnosis of parenchymal defects and grading the severity of small airways disease. *Int J Chron Obstruct Pulmon Dis* 2017; 12: 1579–1587.

21. Jogi J, Jonson B, Ekberg M, *et al.* Ventilation-perfusion SPECT with Tc-99m-DTPA versus Technegas: a head-to-head study in obstructive and nonobstructive disease. *J Nucl Med* 2010; 51: 735–741.

22. Dhawan RT, Gopalan D, Howard L, *et al.* Beyond the clot: perfusion imaging of the pulmonary vasculature after COVID-19. *Lancet Respir Med* 2021; 9: 107–116.

23. Cobes N, Guernou M, Lussato D, *et al.* Ventilation/perfusion SPECT/CT findings in different lung lesions associated with COVID-19: a case series. *Eur J Nucl Med Mol Imaging* 2020; 47: 2453–2460.

24. Zuckier LS. To everything there is a season: taxonomy of approaches to the performance of lung scintigraphy in the era of COVID-19. *Eur J Nucl Med Mol Imaging* 2021; 48: 666–669.

25. Bahloul A, Verger A, Mandry D, *et al.* Signs of tracheobronchitis may constitute the principal finding on the lung SPECT/CT images of COVID-19 patients. *Eur J Nucl Med Mol Imaging* 2021; 48: 2525–2530.

26. Arce VM and Costoya JA. SARS-CoV-2 infection in K18-ACE2 transgenic mice replicates human pulmonary disease in COVID-19. *Cell Mol Immunol* 2021; 18: 513–514.

27. Le Guludec D, Menad F, Faraggi M, *et al.* Myocardial sarcoidosis. Clinical value of technetium-99m sestamibi tomoscintigraphy. *Chest* 1994; 106: 1675–1682.

28. Fu F, Lou J, Xi D, *et al.* Chest computed tomography findings of coronavirus disease 2019 (COVID-19) pneumonia. *Eur Radiol* 2020; 30: 5489–5498.

29. Gurewich V, Thomas D, Stein M, *et al.*
Bronchoconstriction in the presence of
pulmonary embolism. *Circulation* 1963; 27:
339–345.

30. Giuntini C. Ventilation/perfusion scan and
dead space in pulmonary embolism: are they
useful for the diagnosis. *Q J Nucl Med* 2001; 45:
281–286.

31. Fernandes CJ, Luppino Assad A-P, Alves-Jr JA,
et al. Pulmonary embolism and gas exchange.
Respiration 2019; 98: 253–262.

32. Lei Y, Zhang J, Schiavon CR, *et al.* SARS-CoV-2
spike protein impairs endothelial function via
downregulation of ACE 2. *Circ Res* 2021; 128:
1323–1326.

33. Herrero R, Sanchez G and Lorente JA. New
insights into the mechanisms of pulmonary edema
in acute lung injury. *Ann Transl Med* 2018; 6: 32.

34. Ackermann M, Verleden SE, Kuehnel M, *et al.*
Pulmonary vascular endothelialitis, thrombosis,
and angiogenesis in Covid-19. *N Engl J Med*
2020; 383: 120–128.